https://doi.org/10.5194/essd-2023-267
Preprint. Discussion started: 26 July 2023

A 12-years long (2010-2021) hydrological and biogeochemical dataset in the Sicily Channel (Mediterranean Sea)

Francesco Placenti[1], Marco Torri[2*], Katrin Schroeder[3], Mireno Borghini[4], Gabriella Cerrati[5], Angela Cuttitta[2], Vincenzo Tancredi[1], Carmelo Buscaino[1], Bernardo Patti[6]

[1]Consiglio Nazionale delle Ricerche - Istituto per lo studio degli impatti Antropici e Sostenibilità in ambiente marino (CNR-IAS), Campobello di Mazara (TP), Italy.
[2]Consiglio Nazionale delle Ricerche – Istituto di Studi sul Mediterraneo (CNR-ISMed), Palermo, Italy.
[3]Consiglio Nazionale delle Ricerche – Istituto di Scienze Marine (CNR-ISMAR), Venice, Italy.
[4]Consiglio Nazionale delle Ricerche – Istituto di Scienze Marine (CNR-ISMAR), La Spezia, Italy
[5]ENEA – Infrastrutture e Servizi – Servizio e Gestioni Centro Santa Teresa (ISER-STE), Santa Teresa, La Spezia, Italy;
[6]Consiglio Nazionale delle Ricerche - Istituto per lo studio degli impatti Antropici e Sostenibilità in ambiente marino (CNR-IAS), Palermo, Italy.

*Corresponding author: marco.torri@cnr.it

ABSTRACT

The data set presented here consists of 273 Conductivity-Temperature-Depth (CTD) stations, as well as 2034 sampled data points in the water column, where dissolved inorganic nutrients have been measured, that were collected during 12 summer oceanographic cruises (BANSIC series) in the Sicily Channel (Central Mediterranean Sea), between 2010 and 2021. The quality of the CTD dataset is ensured by regular sensor calibrations, an accurate control process adopted during the acquisition, processing and post-processing phases. The quality of the biogeochemical dataset is ensured by the adoption to best-practices analytical and sampling methods. This data collection fills up a gap of information in the Sicily Channel, i.e. a key area where complex water mass exchange processes involve the transfer of physical and biogeochemical properties between the Eastern and the Western Mediterranean. The available dataset will be useful to evaluate the long-term variability on a wide spatial scale, supporting studies on the evolution of the Mediterranean circulation and its peculiar biogeochemistry, as well as on the physical and biogeochemical modeling of this area.

INTRODUCTION

The Mediterranean thermohaline circulation drives the transport of water masses and biogeochemical elements in the different basins and sub-basins and, via the Strait of Gibraltar (SG), controls the exchanges with the Atlantic Ocean (The MerMex Group, 2011).

https://doi.org/10.5194/essd-2023-267
Preprint. Discussion started: 26 July 2023

The thermohaline circulation in the Mediterranean Sea (MS) is anti-estuarine and is mainly driven by the balance between the relatively fresh waters entering at the SG and the negative fresh-water budgets over the whole MS (Sorgente et al., 2011). Specifically, the Sicily Channel (SC), due to its particular bathymetric structure and geographic position, plays a key role in modulating the eastward transport of the fresher and superficial (0-150 m) Atlantic Water (AW) and the underlying (200-500 m) westward transport of the salty Intermediate Water (IW) (Schroeder et al., 2017). From its formation area (either in the Levantine sub-basin or in the Cretan Sea), IW spreads westward into the Ionian Sea (IS), with a significant flow northward towards the Adriatic Sea, where it constitutes an important preconditioning agent for the formation of the Adriatic Deep Water (ADW, which forms the bulk of the Eastern Mediterranean Deep Water, or EMDW; e.g., Gačić et al., 2013). When reaching the Western Mediterranean, and in particular its northern part, the IW preconditions the water column also there and makes it prone to the formation of Western Mediterranean Deep Water (WMDW; e.g., Roether et al., 1996). Although the area of the SC is limited at the east and west by two relatively shallow sills (max depths of 350 m and 550 m, respectively), in its central part the bottom depth can reach 1700 m. It is in this deep central trench where e.g., Gasparini et al. (2005) and others studied the evolution of the upper part of the EMDW (or transitional EMDW, i.e. tEMDW) over time, being able to cross the SC and reach the Tyrrhenian Sea along with the IW flow. Several authors, analyzing long time series of temperature and salinity of the deeper waters of the SC, have highlighted a general positive trend albeit characterized by phases of accelerations and multiannual peaks and fluctuations (Gasparini et al., 2005; Gačić et al., 2013; Bonanno et al., 2014; Ben Ismail et al., 2014; Schroeder et al., 2017; Placenti et al., 2022). Furthermore, these trends are significantly faster than those reported for the global ocean intermediate layer (Borghini et al., 2014; Schroeder et al., 2017). In fact, the semi-enclosed nature of the MS, together with its smaller inertia due to the relative short residence time of its water masses, makes it highly reactive to external forcings, identifying it as a ''hotspot'' for climate change (Giorgi, 2006). Consequently, MS is expected to experience environmental impacts that are considerably greater than those in many other places around the world (The MerMex Group, 2011). As regards the peaks, trends and multiannual fluctuations of temperature and salinity observed in the deeper water of the SC, they are probably ascribable to different processes acting at different spatial and temporal scales, such as the passage of the signature of the Eastern Mediterranean Transient (EMT) (Gasparini et al., 2005), the alternation of circulation phases (cyclonic-anticyclonic) of the Northern Ionian Gyre (NIG)

https://doi.org/10.5194/essd-2023-267
Preprint. Discussion started: 26 July 2023

(Gačić et al., 2013; Bonanno et al., 2014; Placenti et al., 2022) and the effects related to warming of the Eastern Mediterranean (Schroeder et al. al., 2017, 2019).

The anti-estuarine circulation, jointly to the superposition of different time scales of variability, intense wintertime atmospheric forcings, NIG reversals and EMT, act also on the distribution of biogeochemical elements (e.g., inorganic nutrients) and productivity of the MS. The very low productivity of the MS is therefore mainly linked both to the anti-estuarine circulation (Krom et al., 2010) and to the chemical speciation of the dissolved P and N. They in fact reflect a switch from less bioavailable chemical forms of P and N entering the Mediterranean Sea to more bioavailable forms leaving it (Powley et al., 2017). Moreover, the export of nutrients through the IW causes the deep waters of the Eastern Mediterranean Sea to be more nutrient depleted than deep water in all other parts of the global ocean (Krom et al., 2005). Another peculiarity still debated is the higher molar NO_3:PO_4 ratio in the deeper water of the MS compared to the “classical” world oceans Redfield ratio, indicating a general P-limited regime, which becomes stronger along a west-to-east gradient (Belgacem et al., 2020). In this context, the aim of this paper is to compile a large dataset of hydrological (temperature, salinity and pressure) and biogeochemical (nitrate, phosphate and silicate) properties from *in situ* data collected between 2010 and 2021 in the SC, filling up a gap of information in a key area of the MS, where the exchange between the two basins is taking place. The available dataset is a valuable tool in support to the evaluation of the long-term variability and evolution of the Mediterranean circulation and water masses, and provides also a useful contribution for the implementation of models aimed at describing the physical-chemical processes occurring in this area. The dataset could also be integrated in the recently published climatology of dissolved inorganic nutrients (Belgacem et al., 2020), to expand its geographic domain.

DATASET AND METHODS

The hydrological and biogeochemical data collection was carried out as part of an ichthyoplankton monitoring and research program implemented by the Italian National Research Council (CNR). This program was set up with the primary purpose of monitoring the spatio-temporal distribution of the early life stages of European anchovy (*Engraulis encrasicolus*) in the SC and of studying its relationship with the environmental variables, in support to the sustainable exploitation of the population by local fisheries. In this context, since 1998 ichthyoplankton oceanographic surveys based on a common sampling grid have been annually carried out during the summer period within the FAO Geographic Sub-Areas (GSAs) 13, 15, 16 and 19. Since 2010, in addition to the meso-

https://doi.org/10.5194/essd-2023-267
Preprint. Discussion started: 26 July 2023

zooplancton sampling, water sampling for the quantification of macro-nutrients has been included in the survey work plan in order to better characterize the biogeochemical characteristics of the water column and study the relationships with the biotic component.

The dataset presented here results from this sampling effort and assembles information from 12 summer oceanographic cruises conducted on board of different research vessels from 2010 to 2021 (R/V "Urania" from 2010 to 2014; R/V "Minerva Uno" from 2015 to 2017; R/V "G. Dallaporta" from 2018 to 2021). Data were integrated into a dataset consisting of 273 CTD-nutrient stations and 2034 data points (Suppl. 1). The stations are arranged along inshore-offshore transects approximately sub perpendicular to the Sicilian coast, aiming at characterizing the oceanographic and biogeochemical features in a key area for the understanding of the complex exchange processes between the Eastern and Western basins (Fig. 1).

https://doi.org/10.5194/essd-2023-267
Preprint. Discussion started: 26 July 2023

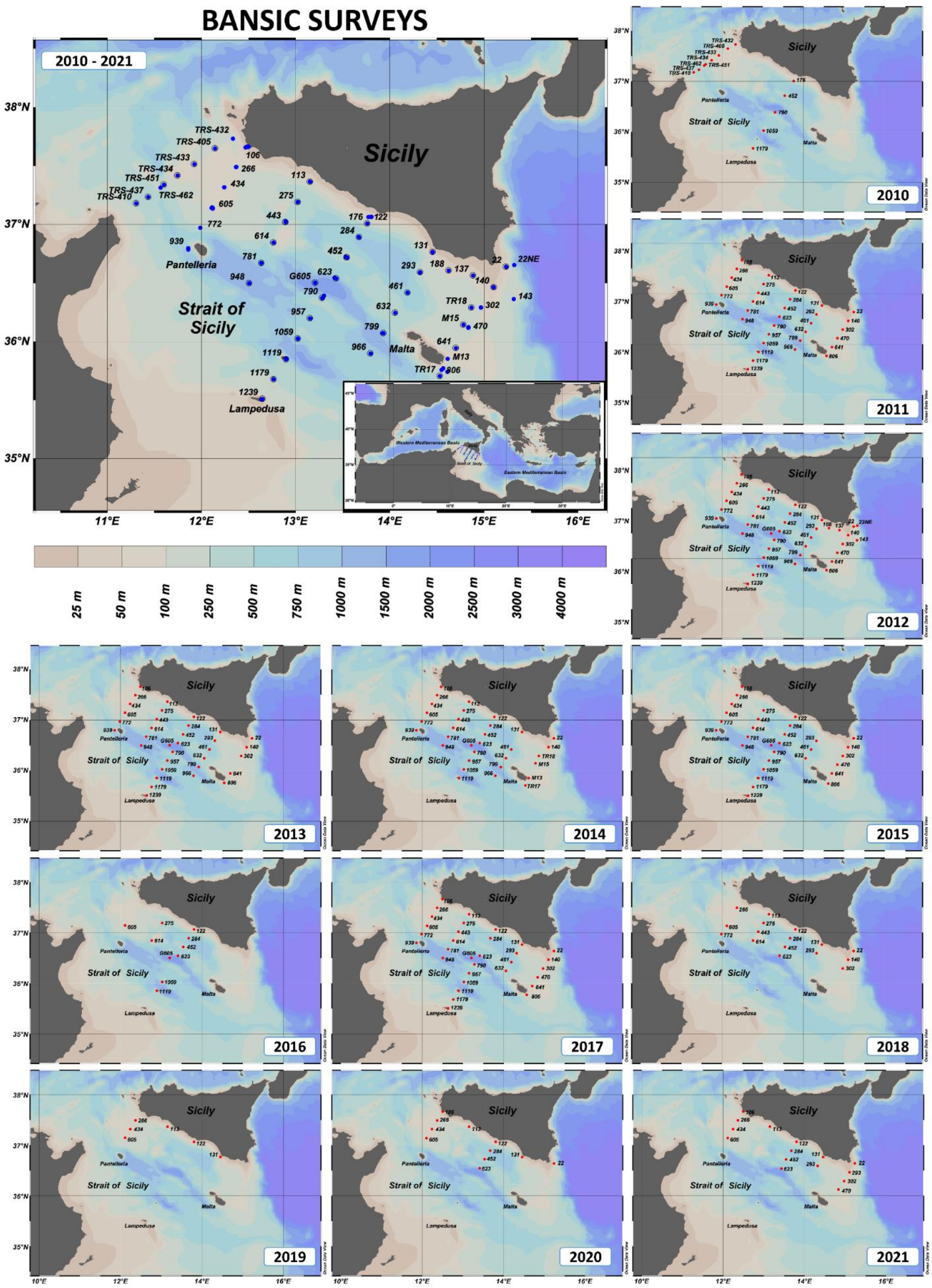

92
93 *Figure 1. Stations map of the Bansic cruises, carried out in the Sicily Strait from 2010 to 2021: CTD*
94 *and nutrient stations are indicated by blue (in the general map) and red circles (in the yearly maps).*
95 *The maps were created using Ocean Data View software (https://odv.awi.de/).*

https://doi.org/10.5194/essd-2023-267
Preprint. Discussion started: 26 July 2023

Hydrological Data Acquisition

At all stations, pressure, salinity, and temperature were measured with a CTD (conductivity, temperature, and depth) probe (Sea-Bird Scientific) mod. SBE 911plus and a General Oceanics rosette with 24 Niskin bottles of 12 L capacity. Temperature measurements were performed with a SBE-3/F thermometer, with a resolution of 0.00015 °C/bit at -1 °C or 0.00018 °C/bit at 31 °C, and conductivity measurements were performed with a SBE-4C sensor, with a resolution of 3 x 10-4 S/m. The vertical profiles of all parameters were obtained by sampling the signals at 24 Hz, with the CTD/rosette going down at a speed of 1 m/s. The rosette is equipped with a sonar altimeter which intercept the bottom 100-70 meters before getting to it. The altimeter is used just for safety, to avoid the rosette to touch the bottom.

Inorganic Nutrient Data Collection

Seawater samples for dissolved inorganic nutrient analysis were collected from the surface to the bottom by means of Niskin bottles. In particular, during the CTD upcast, a variable number of water samples, at selected standard depth, has been considered (surface–25m–50m–75m–100m–150m-200m–300m–400m–500m–600m–700m–800m–900m–1000m–bottom) with slight modifications in the upper layer where significant hydrological variability is typical to occur. All materials used for water sampling on board were earlier conditioned with 10% HCl and rinsed 3 times with ultrapure water. Unfiltered samples were stored on board at –20°C.

Analytical Methods for Inorganic Nutrients

For all cruises, nutrient determination (nitrate, silicate, and phosphate) was carried out following standard colorimetric methods of seawater analysis, defined by Grasshoff et al. (1999) and Hansen and Koroleff (1999) adapted to an automated system. Specifically, the determination of phosphate is based on the colorimetric method, in which a blue color is formed by the reaction of phosphate, molybdate ion and antimony ion, followed by reduction with ascorbic acid. The reduced blue phospho-molybdenum complex is read at 880 nm. Inorganic nitrate is reduced to nitrite at pH 8 in a copperized cadmium reduction coil that reacts with an aromatic amine, leading to the final formation of the azo dye measured at 550 nm. Then, the nitrite that is separately determined must be subtracted from the total amount measured to get the nitrate concentration only. The determination of soluble silicates is based on the reduction of a silico-molybdate complex in acid solution to molybdenum blue by ascorbic acid and the absorbance is measured at 820 nm.

https://doi.org/10.5194/essd-2023-267
Preprint. Discussion started: 26 July 2023

All the analysis of dissolved inorganic nutrients were carried out immediately after each oceanographic cruise, in the nutrient laboratory of the Institute for the Study of Anthropic Impacts and Sustainability in the Marine Environment (CNR-IAS) of Capo Granitola, using the same analytical instrument and the same scientific staff. The concentration (µmol/l) of nitrate, silicate and phosphate was measured by means of a Sial Autoanalyzer ''QUAATRO''. The detection limits for nitrates, silicates and phosphates were 0.02, 0.01 and 0.006 µmol/l, respectively. Even though the use of the same analytical methods, instruments and scientific staff supports the repeatability and the comparison of the measurements, in order to further validate the analytical data, selected seawater samples (sampled in duplicate) have been sent to the nutrient laboratory of nutrients of the Research Center (ENEA) of Santa Teresa (La Spezia), taking advantage on their participation in the framework of the European intercalibration program QUASIMEME (Quality Assurance of Information for Marine Environmental Monitoring in Europe).

The differences in concentrations for all parameters analyzed (nitrates, phosphates and silicates) ranged from 3% to 20%. The differences were greater (10-20%) for concentration values close to the instrumental detection limit and smaller (<10%) at high concentrations. This range of differences is perfectly acceptable considering that ENEA uses a previous generation auto-analyser and that the scientific staff was different. However, we would like to point out that, in both nutrient laboratories, the chemical analyzes were carried out using both the same analytical methods and the same types of reagents.

Quality check of hydrological and nutrient data

The temperature and salinity of the CTD have been regularly calibrated. During 2 cruises, also redundant temperature and salinity sensors were used. When they were available, the secondary sensors have been used to assess the stability of the primary ones.

The temperature and salinity sensors calibrations have been performed before each cruise by CNR technicians at the NATO Centre for Underwater Research (NURC, now Centre for Maritime Research and Experimentation, CMRE) in La Spezia (Italy) until 2016. Between 2017 and 2018 sensors were send to the manufacturer, while since 2019 the calibration is done at the new CNR-ISMAR calibration laboratory in La Spezia (Italy). Table 1 shows a summary of all sensors, their serial numbers and their calibration dates.

Table 1 – Calibration dates and serial numbers of the CTD sensors used during oceanographic cruises.

https://doi.org/10.5194/essd-2023-267
Preprint. Discussion started: 26 July 2023

Cruise	Date	Temp 1		Cond 1		Temp 2		Cond 2	
		sn	cal. date	sn	cal. date	sn	cal. date	sn	cal. date
Bansic 2010	25 Jun–14 Jul 2010	1368	May10	891	May10				
Bansic 2011	08–26 Jul 2011	4440	Apr11	3172	Apr11				
Bansic 2012	04–23 Jul 2012	1183	Nov10	923	Nov10				
Bansic 2013	26 Jun–16 Jul 2013	2810	Oct12	2483	Oct12				
Bansic 2014	22 Jul–9 Aug 2014	4440	Nov13	3172	Nov13				
Bansic 2015	16 Jul–3 Aug 2015	5022	Oct14	3485	Nov14				
Bansic 2016	30 Jun–14 Jul 2016	5022	Oct14	3485	Nov14				
Bansic 2017	13–29 Jun 2017	1183	Jul16	0923	Jun16				
Bansic 2018	07-19 Sep 2018	1142	Aug17	2779	Aug17				
Bansic 2019	30 Sep-12 Oct 2019	1142	Aug17	2779	Feb19	5038	May17	3484	Feb19
Bansic 2020	16-25 Sep 2020	1142	Jan20	2779	Jan20	5038	Jan20	3484	Jan20
Bansic 2021	6-18 Sep 2021	1381	Jun21	1048	Jun21				

After their acquisition, CTD data were pre-processed by the SBE Data Processing™ software, in order to (i) convert the raw data (.hex) to engineering units and store them in a .cnv file, (ii) run a low-pass filter on the data and smooth high frequency data, (iii) align parameter data in time, relative to pressure (to ensure that calculations of salinity and other parameters are made using measurements from the same parcel of water), (iv) remove conductivity cell thermal mass effects from the measured conductivity, (v) compute derived variables, and to (vi) average data, using averaging intervals based on depth range, and split the file into an upcast and a downcast file.

Following the recommendations of the SeaDataNet QC guidelines (SeaDataNet, 2010) The subsequent procedure to assess data quality was based on the following list:

- Check header details (vessel, cruise number, station numbers, date/time, latitude/longitude (start and end), instrument number and type, station depth, cast (up or down)), data type/no. of data points)
- Plot station positions to check not on land
- Check ship speed between stations to look for incorrect position or date/time
- Automatic range checking of each parameter
- Check units of parameters supplied
- Check pressure increasing
- Check no data points below bottom depth
- Plot profiles (individually, in groups, etc)
- Check for spikes
- Check for vertical stability/inversions
- Plot temperature vs. salinity

The resulting dataset is based on the downcast file after selection of averaged data at standard depths corresponding to the water sampling for the inorganic nutrient analysis.

Furthermore, a further control process was carried out taking into account the characteristics of the three water masses identified in the study area, related to 2010-2021 period, and schematized below: a surface layer with a thickness varying over the years, generally less than 150 m of depth and mainly occupied by AW, an intermediate layer (200-500 m) mainly occupied by IW and a deeper layer (>500 m) occupied by the upper part of the DW (Fig. 2h). The first step consisted in the elimination of the outliers from nitrates, phosphates and silicates profiles recorded during annual surveys in each layer. Then, the mean value and the coefficient of variation (CV), i.e., a normalized measure of the dispersion given by the ratio of the standard deviation to the mean, were calculated for each parameter recorded, with the aim of carrying out a comparative control of the occurring patterns.

RESULTS AND DISCUSSION

An analysis was conducted in order to characterize the spatial-temporal trends emerging in the dataset and compare them with the state of the art concerning the study area. In this framework, the vertical distribution pattern of inorganic nutrients in the water column of the SC highlights low concentration values and high variability (Fig. 2; Tab. 2).

https://doi.org/10.5194/essd-2023-267
Preprint. Discussion started: 26 July 2023

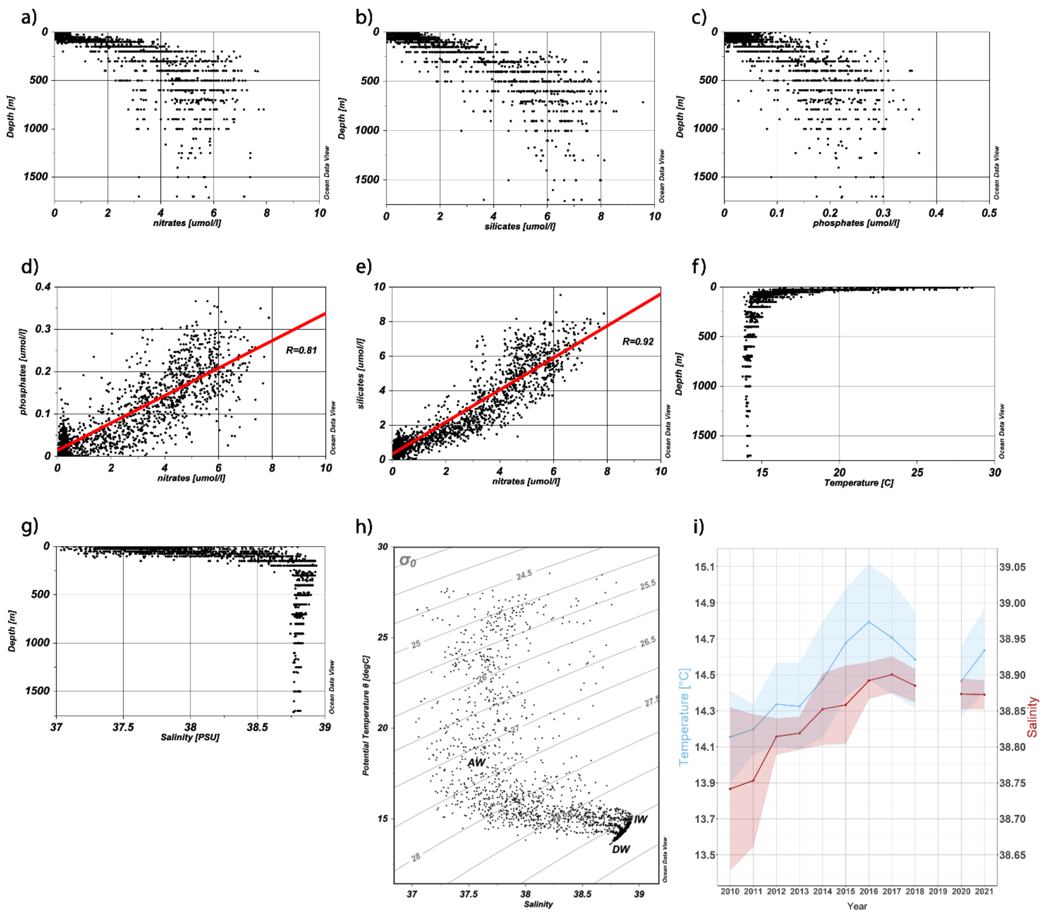

Figure 2. Plots of data on nutrients concentration at selected standard depths along the water column for a) nitrates, b) phosphates, c) silicates; d) N:P and e) N:Si diagrams and related linear regression lines (in red); f) plots of hydrological data at selected standard depths along the water column for temperature and g) salinity (the related colored areas represent the standard deviations); h)potential temperature vs salinity diagram related to 2010-2021 period (AW for Atlantic Water, IW for Intermediate Water and DW for upper Deep Water) and i) time series of annual average values (2010-2021) of temperature (blue line) and salinity (red line) related to the water sampling depths in the IW (200-500 m).

In surface waters the concentration values of inorganic nutrients are close to the instrumental detection limits due to the typical consumption of phytoplankton during the summer period occurring in this layer. This usually results in considerably lower values compared to patterns

https://doi.org/10.5194/essd-2023-267
Preprint. Discussion started: 26 July 2023

observed in the underlying layers (Tab. 2). Moreover, the depth layer 0-150m is characterized by a higher CV due to the pronounced dynamism of the exchange processes affecting the marine ecosystem in this upper part of the water column as well as the interaction with terrestrial sources of nutrients. Specifically, the lowest mean nitrate concentration value of 0.302 µmol/l was measured in BANSIC19 survey, characterized by a quite low number of water samples collected from continental shelf stations only (no data of the intermediate layer are available from 2019 survey), while the highest concentration value of 1.027 µmol/l was measured in BANSIC14 survey (Tab. 2). Regarding the phosphates the lowest mean concentration value was 0.030 µmol/l (BANSIC12) and the highest one 0.064 µmol/l (BANSIC13), while for silicates the mean concentration values ranged from a minimum of 0.608 µmol/l (BANSIC15) to a maximum of 1.173 µmol/l (BANSIC10) (Tab. 2). The lower sampling effort carried out in BANSIC19 also corresponds to a lower variation of nitrates and phosphates compared to the other surveys, while the silicates showed more homogeneous patterns among surveys. Specifically, in the superficial layer CV varied between 0.762 (BANSIC19) and 1.566 (BANSIC20) for nitrates, between 0.471 (BANSIC19) and 1.333 (BANSIC21) for phosphates, and finally between 0.433 (BANSIC20) and 0.83 (BANSIC15) for silicates.

The nutrients that have been consumed at the surface are regenerated in the mesopelagic layer by bacteria and animals (due to respiration), increasing the nutrient concentrations in the deeper water masses over time (e.g., Schroeder et al., 2010). In this way, the intermediate waters of the SC are characterized by higher nutrient concentration values than the overlying layer and lower variability (Fig. 2a-c and Tab. 2). Specifically, mean concentration values in the intermediate waters ranged from 2.976 µmol/l in BANSIC15 to 5.4 µmol/l in BANSIC11 for nitrates, from 2.589 µmol/l (BANSIC15) to 4.86 µmol/l (BANSIC11) for silicates, and from 0.095 µmol/l in BANSIC18 to 0.204 µmol/l in 2021 for phosphates (Tab. 2).

Regarding the dispersion of the values in this layer, nitrates CV ranged between 0.0068 (BANSIC20) and 0.319 (BANSIC21), phosphates CV ranged between 0.171 (BANSIC20) and 0.585 (BANSIC16), and silicates CV ranged between 0.161 (BANSIC20) and 0.528 (BANSIC15) (Tab. 2).

In the trench of the SC, the deep layer (see section >500m-bottom of Tab. 2) is characterized by mean concentration values more homogeneous over years than in the above layers. There, the lowest mean concentration values for nitrates and silicates (4.13 and 4.701 µmol/l) were measured in BANSIC15, while the lowest value for phosphates (0.097 µmol/l) was measured during BANSIC10. The highest mean values of nitrates (5.861 µmol/l), phosphates (0.241 µmol/l) and silicates (6.474 µmol/l) were respectively measured during BANSIC11, BANSIC17-21 and BANSIC13. Similarly, the

https://doi.org/10.5194/essd-2023-267
Preprint. Discussion started: 26 July 2023

Open Access Earth System Science Data Discussions

deep layer is characterized by the lowest variability in nutrient concentrations. Indeed, the nitrate CV varied between 0.0058 (BANSIC10) and 0.299 (BANSIC21), between 0.07 (BANSIC20) and 0.339 (BANSIC10) for the phosphates and between 0.029 (BANSIC20) and 0.277 (BANSIC15) for the silicates.

The molar ratios of nitrate:phosphate (N:P) and silicate:nitrate (Si:N) in the whole water column of the SS show high correlation coefficients (R=0.81 and 0.92, respectively) (Fig. 2d,e). Specifically, in the surface layer (0-150m) the mean values of N:P and Si:N over the period 2010-2021 are equal to 18 and 1.4 respectively, which become 31 and 0.9 in the intermediate layer (200-500m) and 29 and 1.1 in the deep layer (500m-bottom), in agreement with Ribera D'Alcalà et al. (2003) and with Placenti et al. (2013; 2022). Observed N:P values are higher than the classical Redfield ratio (16:1). The high N:P ratio can result from either a decrease in phosphate or an increase in nitrate; however, the reason of this anomaly is still unclear (e.g., Schroeder et al., 2010). Among the various hypotheses, we agree about the possible role of external inputs, together with very limited denitrification (Krom et al., 2010; Huertas et al., 2012; Van Cappellen et al., 2014), in explaining the observed very high NO_3:PO_4 ratios in the deeper water (Powley et al., 2017).

Table 2. Average values of concentration and coefficients of variation (CV) of both physical (temperature and salinity) and chemical (nitrates, phosphates and silicates) parameters in the 12 oceanographic surveys carried out yearly over the period 2010-2021 reported in this paper, by depth layer (superficial 0-150m, intermediate 200-500m and deep >500m-bottom).

Cruise name	Sampling date	Research vessel name	Station number	Max. Sampling depth [m]	Sample number	Nitrates		Phosphates		Silicates		Temperature		Salinity	
						mean [umol/l]	CV	mean [umol/l]	CV	mean [umol/l]	CV	mean [°C]	CV	mean [psu]	CV
Layer 0-150 m															
Bansic10	25 June–14 Jul 2010	Urania	13	700	62	0.743	1.172	0.043	1.009	1.173	0.697	17.477	0.148	37.610	0.011
Bansic11	08–26 Jul 2011	Urania	34	1130	154	0.736	1.446	0.034	0.831	1.002	0.686	18.574	0.234	37.978	0.0087
Bansic12	04–23 Jul 2012	Urania	39	1711	203	0.707	1.066	0.030	0.954	1.037	0.478	17.923	0.237	38.177	0.0117
Bansic13	26 June–16 Jul 2013	Urania	34	1700	178	0.835	1.302	0.064	0.727	1.061	0.628	17.380	0.175	37.919	0.0094
Bansic14	22 Jul–9 Aug 2014	Urania	32	1700	164	1.027	1.116	0.051	0.803	0.940	0.703	17.997	0.201	37.872	0.0123
Bansic15	16 Jul–3 Aug 2015	Minerva Uno	31	1700	158	0.681	1.117	0.036	0.893	0.608	0.833	18.313	0.240	38.206	0.0093
Bansic16	30 June–14 Jul 2016	Minerva Uno	10	1700	51	0.777	1.237	0.043	0.638	0.614	0.690	17.673	0.176	37.812	0.0135
Bansic17	13–29 June 2017	Minerva Uno	32	1700	160	0.898	1.015	0.037	1.037	1.043	0.538	17.880	0.179	37.956	0.0125
Bansic18	07-19 Sept 2018	G. Dallaporta	16	700	77	0.957	1.286	0.039	0.671	1.150	0.649	18.646	0.229	38.091	0.0118
Bansic19	30 Sept-12 Oct 2019	G. Dallaporta	6	72	21	0.302	0.762	0.040	0.471	0.721	0.605	19.784	0.189	38.037	0.0068
Bansic20	16-25 Sept 2020	G. Dallaporta	11	1000	44	0.596	1.566	0.032	0.697	1.083	0.433	19.861	0.222	38.091	0.0096

https://doi.org/10.5194/essd-2023-267
Preprint. Discussion started: 26 July 2023

Bansic21	6-18 Sept 2021	G. Dallaporta	15	996	67	0.577	1.449	0.073	1.333	1.087	0.526	19.623	0.222	37.822	0.0128
Layer 200-500 m															
Bansic10	25 June–14 Jul 2010	Urania	13	700	26	4.086	0.238	0.166	0.445	4.606	0.309	14.155	0.018	38.742	0.0029
Bansic11	08–26 Jul 2011	Urania	34	1130	65	5.400	0.273	0.135	0.443	4.860	0.364	14.196	0.010	38.753	0.0024
Bansic12	04–23 Jul 2012	Urania	39	1711	68	4.407	0.244	0.170	0.342	4.443	0.342	14.336	0.016	38.814	0.0007
Bansic13	26 June–16 Jul 2013	Urania	34	1700	65	4.473	0.216	0.163	0.338	4.623	0.271	14.325	0.017	38.819	0.0006
Bansic14	22 Jul–9 Aug 2014	Urania	32	1700	61	4.753	0.194	0.178	0.298	4.047	0.307	14.474	0.022	38.852	0.0013
Bansic15	16 Jul–3 Aug 2015	Minerva Uno	31	1700	57	2.976	0.402	0.148	0.476	2.589	0.528	14.677	0.020	38.858	0.0014
Bansic16	30 June–14 Jul 2016	Minerva Uno	10	1700	23	4.002	0.277	0.096	0.585	3.097	0.416	14.794	0.022	38.892	0.0007
Bansic17	13–29 June 2017	Minerva Uno	32	1700	52	4.017	0.290	0.167	0.397	4.193	0.294	14.705	0.021	38.900	0.0006
Bansic18	07-19 Sept 2018	G. Dallaporta	16	700	16	4.460	0.142	0.095	0.520	4.223	0.185	14.584	0.018	38.885	0.0006
Bansic19	30 Sept-12 Oct 2019	G. Dallaporta	6	72											
Bansic20	16-25 Sept 2020	G. Dallaporta	11	1000	11	4.301	0.068	0.115	0.171	3.869	0.161	14.464	0.013	38.873	0.0006
Bansic21	6-18 Sept 2021	G. Dallaporta	15	996	13	5.025	0.319	0.204	0.304	4.677	0.254	14.634	0.016	38.872	0.0005
Layer >500-bottom															
Bansic10	25 June–14 Jul 2010	Urania	13	700	4	4.420	0.006	0.097	0.339	4.987	0.045	13.908	0.004	38.777	0.0002
Bansic11	08–26 Jul 2011	Urania	34	1130	25	5.861	0.125	0.179	0.280	6.392	0.163	13.946	0.003	38.787	0.0002
Bansic12	04–23 Jul 2012	Urania	39	1711	49	5.413	0.171	0.216	0.217	6.468	0.163	13.997	0.005	38.780	0.0003
Bansic13	26 June–16 Jul 2013	Urania	34	1700	39	4.886	0.158	0.207	0.212	6.474	0.150	14.019	0.003	38.794	0.0002
Bansic14	22 Jul–9 Aug 2014	Urania	32	1700	37	5.546	0.106	0.239	0.190	6.088	0.127	14.069	0.003	38.811	0.0003
Bansic15	16 Jul–3 Aug 2015	Minerva Uno	31	1700	26	4.130	0.240	0.238	0.267	4.701	0.277	14.125	0.003	38.817	0.0003
Bansic16	30 June–14 Jul 2016	Minerva Uno	10	1700	16	5.774	0.240	0.118	0.339	6.180	0.237	14.222	0.006	38.834	0.0005
Bansic17	13–29 June 2017	Minerva Uno	32	1700	25	4.954	0.231	0.241	0.203	6.205	0.117	14.229	0.003	38.837	0.0003
Bansic18	07-19 Sept 2018	G. Dallaporta	16	700	3	5.315	0.036	0.159	0.093	5.905	0.084	14.200	0.003	38.832	0.0003
Bansic19	30 Sept-12 Oct 2019	G. Dallaporta	6	72											
Bansic20	16-25 Sept 2020	G. Dallaporta	11	1000	7	4.650	0.017	0.155	0.070	5.038	0.030	14.201	0.003	38.834	0.0002
Bansic21	6-18 Sept 2021	G. Dallaporta	15	996	7	5.474	0.299	0.241	0.279	6.229	0.191	14.248	0.003	38.815	0.0002

As far as the hydrological properties of the water masses in the study area, it is worth noting that over the (summer) period 2010-2021 in the surface layer the average temperature varied in the range 17.380-19.861 °C, with a general increasing trend peaking in 2020. Similarly, the salinity showed increasing values in the range 37.610-38.206 with a peak of in 2015 (Tab. 2). This layer is characterized by a strong interannual and spatial variability as subject to continuous interaction with the atmosphere, as also highlighted by one or two higher orders of magnitude in CV values of physical parameters in the superficial layer compared to the deeper layers (Fig. 2f, g; Tab. 2). Indeed,

https://doi.org/10.5194/essd-2023-267
Preprint. Discussion started: 26 July 2023

in the upper layer the CV of temperature varied between 0.148 (BANSIC10) and 0.240 (BANSIC15), and the CV of salinity ranged between 0.007 (BANSIC19) and 0.014 (BANSIC16).

Instead, the deeper water masses, with their lower variability in heat and salt content turn out to be much more suitable for monitoring any changes over long periods. In the IW layer the CV of temperature ranged between 0.013 (BANSIC20) and 0.022 (BANSIC14 and BANSIC16), while the CV of salinity ranged between 0.0005 (BANSIC21) and 0.0029 (BANSIC10) (Tab. 2). Values of temperature in our time series (2010-2021) shows an increase in average values of about 0.5 °C (14.155-14.634 °C), with a peak of 14.794 in 2017 (Tab. 2). Similarly, the corresponding increase in salinity was about 1.15 psu (37.742-38.885) with a peak of 38.900 psu reached in 2018 (Tab. 2). Similar trends have been also highlighted in the same area by Schroeder et al. (2017) and related to the increase to drying processes affecting the surface waters from which the LIW originates. Within the time series (2010-2021) two patterns can be distinguished, the first (2010-2016) is characterized by an average annual increase in temperature (dT/dt) of about 0.1 °C/year, the second one (2017-2020) by an annual decrease in temperature of 0.08 °C/year (Fig. 2i; Tab. 2). Finally, in 2021 a slight rise in temperature occurred (Fig. 2i; Tab. 2). Similarly, the salinity patterns show an average annual increase (dS/dt) of 0.022 over the period 2010-2016 and an annual decrease of 0.007 afterwards (2017-2021) (Fig. 2i; Tab. 2). A recent study advanced hypotheses on a possible link between the temperature and salinity positive trends over the period 2010-2016 and the anticyclonic phase of the NIG over the years 2006-2010, while the negative trends over the period 2017-2021 have been connected to the cyclonic phase of the NIG during years 2011-2016 (Placenti et al., 2022).

Conversely, the nitrates and silicates mean annual concentrations show a slight decrease up to 2015-2016 and then slight increase until 2021 (Tab. 2), in agreement with the state of the art regarding the SS (Placenti et al., 2022).

The DW are characterized by very low values in CV of both temperature and salinity (between 0.003-0.006 and 0.002-0.005, respectively) with very slight differences across the yearly surveys (Tab. 2). Moreover, the average annual temperature and salinity slightly increased from 2010 until 2017 (13.908-14.299 °C and 38.777-38.837), and then slightly decreased until 2020 (Tab. 2). On the contrary, the patterns of nitrates and silicates would appear to be characterized by a slight decrease (5.861-4.130 and 6.392-4.701 µmol/l) between 2011 and 2015 and by a slight discontinuous increase afterwards until 2021 (Tab. 2).

DATA AVAILABILITY

https://doi.org/10.5194/essd-2023-267
Preprint. Discussion started: 26 July 2023

Dataset and metadata are available as a *.csv merged file and *xlsx format respectively from ZENODO and will be accessed in full open access form at https://doi.org/10.5281/zenodo.8125006 (Placenti et al., 2023) after acceptance.

CONCLUSION

The dataset described here has the advantage of having been collected within the same monitoring program implemented on an important area of the Mediterranean Sea. Over time, the data has been collected consistently by the same technicians and researchers, who have been able to apply a rigorous quality check during both field and laboratory activities. This made it possible to minimize any biases deriving from the different experience of the personnel and from the use of different types of instrumentation and protocols. The spatial and temporal variability that characterizes this dataset therefore reliably reflects the effect of environmental processes that occurred in the marine environment, making this dataset usable for different fields of application. In support to this, the analysis of the mean values and of the variability of the parameters along the water column and among different surveys showed an agreement with the patterns commonly recognized in the marine environment and highlighted in other datasets collected in different areas of the Mediterranean Sea. Moreover, the analysis shown in this paper is highly consistent with the trends evidenced in the literature concerning the Sicily Channel. In this framework, the availability of this dataset to the scientific community fills an important lack in field observations of a crucial area, the Sicily Channel, where exchanges between the western and eastern Mediterranean basin take place, providing support to studies aimed at describing the ongoing processes as well as at realizing reliable projections regarding the effects of these processes in the near future.

AUTHOR CONTRIBUTIONS

FP wrote the manuscript and analyzed the dataset. MT wrote the manuscript and prepared the figures. VT and CB participated to the fieldwork and laboratory analyses. KS wrote the manuscript and improved the quality check of the oceanographic data. GC, AC and BP coordinated the field work and the laboratory analyses and supervised the writing of the text. MB managed the technical aspects related to the oceanographic instrumentation for the acquisition of the hydrological parameters and helped with specific technical aspects of the manuscript. All authors contributed to the article and approved the submitted version.

COMPETING INTERESTS

The authors declare that they have no conflict of interest.

FINANCIAL SUPPORT

This study was mainly supported by the Italian National Research Council (CNR) through USPO office and by the FAO Regional Project MedSudMed "Assessment and Monitoring of the Fishery Resources and the Ecosystems in the Straits of Sicily", co-funded by the Italian Ministry MIPAAF through the Directorate General for Maritime Affairs and Fisheries of the European Commission (DG MARE). Other national research programmes supported this study including project SSD-PESCA, coordinated by the Ministry of the Education, University and Research (MIUR) and founded by the Ministry of Economic Development (MISE), and the Flagship Project RITMARE – The Italian Research for the Sea, coordinated by the Italian National Research Council and funded by MIUR.

ACKNOWLEDGMENTS

Masters of the Urania, Minerva Uno, Dallaporta and all their crew are thanked for their work in support to the sampling activities during the oceanographic cruises. We are grateful to Carmelo Bennici, Girolama Biondo, Gaspare Buffa, Ignazio Fontana, Giovanni Giacalone, Luigi Giaramita, Marianna Musco, Carlo Patti and Giorgio Tranchida for their valuable technical support and the sampling collection during the oceanographic surveys.

REFERENCES

Belgacem, M., Chiggiato, J., Borghini, M., Pavoni, B., Cerrati, G., Acri, F., Cozzi, S., Ribotti, A., Álvarez, M., Lauvset, S. K., and Schroeder, K.: Dissolved inorganic nutrients in the western Mediterranean Sea (2004–2017), Earth Syst. Sci. Data, 12, 1985–2011, 2020, https://doi.org/10.5194/essd-12-1985-2020, 2020.

Ben Ismail, S., Schroeder, K., Sammari, C., Gasparini, G. P., Borghini, M., and Aleya, L.: Interannual variability of water mass properties in the Tunisia-Sicily Channel, J. Mar. Syst., 135, 14–28, 2014.

Bonanno, A., Placenti, F., Basilone, G., Mifsud, R., Genovese, S., Patti, B., Di Bitetto, M., Aronica, S., Barra, M., Giacalone, G., Ferreri, R., Fontana, I., Buscaino, G., Tranchida, G., Quinci E., and Mazzola, S.: Variability of water mass properties in the Strait of Sicily in summer period of 1998–2013, Ocean Sci.10:759–770, 2014.

Borghini, M., Bryden, H., Schroeder, K., Sparnocchia, S., and Vetrano, A.: The Mediterranean is becoming saltier, Ocean Sci. 10, 693–700, http://dx.doi.org/10.5194/os-10-693-2014, 2014.

https://doi.org/10.5194/essd-2023-267
Preprint. Discussion started: 26 July 2023

Gačić, M., Schroeder, K., Civitarese, G., Cosoli, S., Vetrano, A., and Borzelli, G.L.E.: Salinity in the Sicily channel corroborates the role of the Adriatic-Ionian bimodal oscillating system (BiOS) in shaping the decadal variability of the Mediterranean overturning circulation, Ocean Sci. 9, 83–90, https://doi.org/10.5194/os-9-83-2013, 2013.

Gasparini, G.P., Ortona, A., Budillon, G., Astraldi, M., and Sansone, E.: The effect of the Eastern Mediterranean Transient on the hydrographic characteristics in the Strait of Sicily and in the Tyrrhenian Sea, Deep-Sea Res. I Oceanogr. Res. Pap. 52 (6), 915–935, 2005.

Grasshoff, K., Kremling, K., and Ehrhardt, M.: Methods of Seawater Analysis. Wiley-Vch Verlag, Weinheim, 1999.

Hansen, H. P. and Koroleff, F.: Determination of nutrients, Methods of Seawater Analysis, 10, 159–228, 1999.

Huertas, I.E., Rios, A.F., Garcia-Lafuente, J., Navarro, G., Makaoui, A., Sanchez-Roman, A., Rodriguez-Galvez, S., Orbi, A., Ruiz, J., and Perez, F.F.: Atlantic forcing of the Mediterranean oligotrophy, Glob. Biogeochem. Cycles 26, GB2022, http://dx.doi.org/10.1029/2011GB004167, 2012.

Krom, M.D., Woodward, E.M.S., Herut, B., Kress, N., Carbo, P., Mantoura, R.F.C., Spyres, G., Thingstad, T.F., Wassmann, P., Wexels Riser, C., Kitidis, V., Law, C.S., and Zodiatis, G.: Nutrient cycling in the south east Levantine basin of the Eastern Mediterranean: results from a phosphorus starved system, Deep-Sea Res. II 52 (22–23), 2879–2896, 2005.

Krom, M. D., Emeis, K. C., and Van Cappellen, P.: Why is the eastern Mediterranean phosphorus limited? Prog. Oceanogr., 85(3–4), 236–244, http://dx.doi.org/10.1016/j.pocean.2010.03.003, 2010.

Placenti, F., Schroeder, K., Bonanno, A., Zgozi, S., Sprovieri, M., Borghini, M, Rumolo, P., Cerrati, G., Bonomo, S., Genovese, S., Basilone, G., Haddoud, D. A., Patti, B., El Turki, A., Hamza, M., and Mazzola, S.: Water masses and nutrient distribution in the Gulf of Syrte and between Sicily and Libya, J. Marine Sys., 121–122, 36–46, 2013, http://dx.doi.org/10.1016/j.jmarsys.2013.03.012, 2013.

Placenti, F., Torri, M., Pessini, F., Patti, B., Tancredi, V., Cuttitta, A., Giaramita, L., Tranchida, G., and Sorgente, R.: Hydrological and biogeochemical patterns in the Sicily Channel: new insights from the last decade (2010-2020), Front. Mar. Sci. 9, https://doi.org/10.3389/fmars.2022.733540, 2022.

Placenti, F., Torri, M., Borghini, M., Cerrati, G., Cuttitta, A., Tancredi, V., Buscaino, C., and Patti, Bernardo. New hydrological-biogeochemical dataset (2010-2021) in the Strait of Sicily [Data set and metadata]. Zenodo. https://doi.org/10.5281/zenodo.8125006, 2023.

Powley, H.R., Krom, M.D., and Van Cappellen, P.: Understanding the unique biogeochemistry of the Mediterranean Sea: insights from a coupled phosphorus and nitrogen model Glob. Biogeochem. Cycles, 31, pp. 1010-1031, 10.1002/2017GB005648, 2017.

Redfield, A.C., Ketchum, B.H., and Richards, F.A.: The influence of organisms on the composition of sea water, In: Hill, M.N. (Ed.), The Sea, vol. 2. Interscience, New York, pp. 224–228, 1963.

Ribera D'Alcalà, M., Civitarese, G., Conversano, F., and Lavezza, R.: Nutrient ratios and fluxes hint at overlooked processes in the Mediterranean Sea, J. Geophys. Res.,108(C9),8106, doi:10.1029/2002JC0016500, 2003.

Roether, W., Manca, B.B., Klein, B., Bregant, D., Georgopoulos, D., Beitzel, V., Kovacevic ́, V., and Luchetta, A.: Recent changes in eastern mediterranean deep waters, Science 271 (5247), 333–335, http://dx.doi.org/10.1126/science, 1996.

Schroeder, K., Gasparini, G. P., Borghini, M., Cerrati, G., and Delfanti, R.: Biogeochemical tracers and fluxes in the Western Mediterranean Sea, spring 2005, J. Mar. Syst. 80, 8–24, doi: 10.1016/j.jmarsys.2009.08.002, 2010.

Schroeder, K., Chiggiato, J., Josey, S. A., Borghini, M., Aracri, S., and Sparnocchia, S.: Rapid response to climate change in a marginal sea. Sci. Rep. 7:4065, doi: 10.1038/s41598-017-04455-5, 2017.

Schroeder, K., Chiggiato, J., Ben Ismail, S., Borghini, M., Patti, B. and Sparnocchia, S.: Mediterranean deep and intermediate water mass properties. In: Copernicus Marine Service Ocean State Report, Issue 3, Journal of Operational Oceanography, 12:sup1, s26–s30; doi: 10.1080/1755876X.2019.16330, 2019.

Sorgente, R., Olita, A., Oddo, P., Fazioli, L., and Ribotti, A.: Numerical simulation and decomposition of kinetic energy in the Central Mediterranean: insight on mesoscale circulation and energy conversion, Ocean Sci., 7, 503–519, doi: 10.5194/os-7-503-2011, 2011.

The Mermex group: Durrieu de Madron, X., Guieu, C., Sempéré, R., Conan, P., Cossa, D., D'Ortenzio, F., Estournel, C., Gazeau, F., Rabouille, C., Stemmann, L., Bonnet, S.,Diaz, F., Koubbi, P., Radakovitch, O., Babin, M., Baklouti, M., Bancon-Montigny, C.,Belviso, S., Bensoussan, N., Bonsang, B., Bouloubassi, I., Brunet, C., Cadiou, J.-F.,Carlotti, F., Chami, M., Charmasson, S., Charrière, B., Dachs, J., Doxaran, D., Dutay,J.-C., Elbaz-Poulichet, F., Eléaume, M., Eyrolles, F., Fernandez, C., Fowler, S.,Francour, P., Gaertner, J.C., Galzin, R., Gasparini, S., Ghiglione, J.-F., Gonzalez, J.-L.,Goyet, C., Guidi, L., Guizien, K., Heimbürger, L.-E., Jacquet, S.H.M., Jeffrey, W.H.,Joux, F., Le Hir, P., Leblanc, K., Lefèvre, D., Lejeusne, C., Lemé, R., Loÿe-Pilot, M.-D.,Mallet, M., Méjanelle, L., Mélin, F., Mellon, C., Mérigot, B., Merle, P.-L., Migon, C.,Miller, W.L., Mortier, L., Mostajir, B., Mousseau, L., Moutin, T., Para, J., Pérez, T.,Petrenko, A., Poggiale, J.-C., Prieur, L., Pujo-Pay, M., Pulido-Villena, Raimbault, P.,Rees, A.P., Ridame, C., Rontani, J.-F., Ruiz Pino, D., Sicre, M.A., Taillandier, V.,Tamburini, C., Tanaka, T., Taupier-Letage, I., Tedetti, M., Testor, P., Thébault, H.,Thouvenin, B., Touratier, F., Tronczynski, J., Ulses, C., Van Wambeke, F.,Vantrepotte, V., Vaz, S., Verney, R.: Marine ecosystems'responses to climatic and anthropogenic forcings in the Mediterranean, Prog. Oceanogr., 91. doi:10.1016/j.pocean.2011.02.003.T, 2011.

SeaDataNet: Data Quality Control Procedures, 6th Framework of EC DG Research, Version 2.0, May 2010, https://www.seadatanet.org/Standards/Data-Quality-Control, 2010

Stansfield, K., Gasparini, G.P., and Smeed, D.A.: High-resolution observations of the path of the overflow from the Sicily Strait, Deep Sea Res., Part I, 50, 1129–1149, 2003.

https://doi.org/10.5194/essd-2023-267
Preprint. Discussion started: 26 July 2023

Van Cappellen, P., Powley, H. R., Emeis, K.-C., and Krom, M. D.: A biogeochemical model for phosphorus and nitrogen cycling in the eastern Mediterranean Sea (EMS), Part 1. Model development, initial conditions and sensitivity analyses, J. Mar. Syst., 139, 460–471, 2014.